

Materials Research Letters

ISSN: 2166-3831 (Online) Journal homepage: www.tandfonline.com/journals/tmrl20

Revealing interfacial diffusion kinetics in ultra-fine-laminated Ni with low-angle grain boundaries

Z. B. Wang, S. V. Divinski, Z. P. Luo, Y. Buranova, G. Wilde & K. Lu

To cite this article: Z. B. Wang, S. V. Divinski, Z. P. Luo, Y. Buranova, G. Wilde & K. Lu (2017) Revealing interfacial diffusion kinetics in ultra-fine-laminated Ni with low-angle grain boundaries, Materials Research Letters, 5:8, 577-583, DOI: 10.1080/21663831.2017.1368036

To link to this article: https://doi.org/10.1080/21663831.2017.1368036

© 2017 The Author(s). Published by Informa UK Limited, trading as Taylor & Francis Group.

Published online: 23 Aug 2017.

Submit your article to this journal

Article views: 1738

View related articles

View Crossmark data

Citing articles: 3 View citing articles

Full Terms & Conditions of access and use can be found at
https://www.tandfonline.com/action/journalInformation?journalCode=tmrl20

MATER. RES. LETT., 2017
VOL. 5, NO. 8, 577–583
https://doi.org/10.1080/21663831.2017.1368036

MATERIALS RESEARCH LETTERS
Taylor & Francis
Taylor & Francis Group

ORIGINAL REPORT

OPEN ACCESS Check for updates

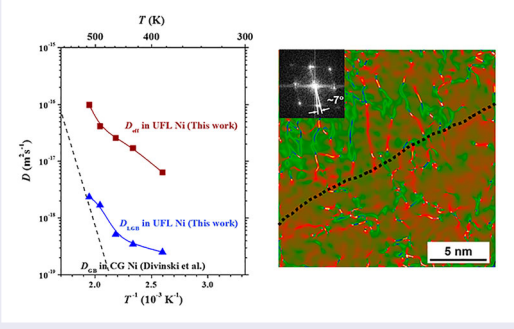
Revealing interfacial diffusion kinetics in ultra-fine-laminated Ni with low-angle grain boundaries

Z. B. Wang[a], S. V. Divinski[b], Z. P. Luo[a], Y. Buranova[b], G. Wilde[b] and K. Lu[a]

[a]Shenyang National Laboratory for Materials Science, Institute of Metal Research, Chinese Academy of Sciences, Shenyang, People's Republic of China; [b]Institute of Materials Physics, University of Münster, Münster, Germany

ABSTRACT

An ultra-fine-laminated (UFL) Ni sample with a high fraction of low-angle grain boundaries (LAGBs) was produced by dynamic plastic deformation. And self-diffusion behavior was studied in this material by the radio-tracer technique. Significantly enhanced interfacial diffusivity was detected in the UFL Ni in comparison with coarse-grained Ni. Analyses indicated that diffusion along LAGBs in the UFL sample is unexpectedly faster than the typical diffusion rates along conventional grain boundaries in the coarse-grained sample. This behavior is explained by the interaction of LAGBs with numerous extrinsic dislocations, as revealed by high-resolution transmission electron microscopy.



ARTICLE HISTORY
Received 20 June 2017

KEYWORDS
Ultra-fine laminated; dynamic plastic deformation; Ni; diffusion; low-angle grain boundary

IMPACT STATEMENT

This work is the first to demonstrate that low-angle grain boundaries in ultra-fine-laminated Ni possess extremely fast diffusion rate, which contributes to understanding the role of interfaces in nanostructured metals.

Introduction

Tailoring the number of interfaces and their structure and/or their distribution is the key to optimize physical and chemical properties of nanostructured materials, as well as to achieve synergies of different properties [1,2]. At increased strain rates of $10^2-10^3\,s^{-1}$, a smaller boundary spacing with a much higher fraction of low-angle grain boundaries (LAGBs) is formed in Ni in comparison with that formed at lower strain rates [3]. Previous studies showed that nano-laminated or ultra-fine laminated (UFL) structures possess a combination of high strength and high stability, because a network of LAGBs is both effective in resisting dislocation movement and presents a low-energy state [1,4]. For example, the hardness of nanolaminated Ni (~20 nm in layer thickness) is ~6.4 GPa, which is higher than any value reported for pure Ni processed by severe plastic deformation (SPD) methods. Additionally, the onset temperature for thickening of the nanolaminates is ~60 K higher than the coarsening temperature of nanograined Ni with a comparable grain size.

Interfacial diffusion studies have been developed as an alternative method to characterize the interfaces in nanostructured materials, in which a large number of interfaces exist, enabling reliable measurements of pure interfacial diffusion at rather low homologous temperatures [5–7] (i.e. in the strict C-type kinetic regime after Harrison's classification [8]). Moreover, tracer diffusion

CONTACT Z. B. Wang zbwang@imr.ac.cn Shenyang National Laboratory for Materials Science, Institute of Metal Research, Chinese Academy of Sciences, 72 Wenhua Road, Shenyang 110016, People's Republic of China

© 2017 The Author(s). Published by Informa UK Limited, trading as Taylor & Francis Group.
This is an Open Access article distributed under the terms of the Creative Commons Attribution License (http://creativecommons.org/licenses/by/4.0/), which permits unrestricted use, distribution, and reproduction in any medium, provided the original work is properly cited.

measurements have turned out to be an extremely sensitive probe of structural changes at interfaces induced by deformation [9]. Most results showed that under certain conditions, the interfaces, including grain boundaries (GBs) and twin boundaries (TBs), possess much higher diffusivities in SPD metals with respect to those in coarse-grained samples [5,10–12]. Such enhancements were related to their deformed state due to the increased number of extrinsic dislocations and an excess free volume located at such interfaces. This results in a higher free energy state compared with conventional ones in coarse-grained samples. Is it possible that the basic transport properties of LAGBs, in fact of just a simple array of equidistant dislocations in a simplest case, could be modified via an intensive interaction with deformation-induced dislocations? This is the central issue of the present report.

In the present study, a UFL Ni sample with a high fraction of LAGBs was produced, and intergranular diffusion was studied at low homologous temperatures, so that lattice diffusion was negligible. Subsequently, the diffusion flux along LAGBs and the structural characteristics of the interfaces were carefully measured and analyzed.

Experimental details

A cylindrical Ni sample ($\sim$99.96 wt.% in purity) with a diameter of 20 mm and a height of 27.2 mm was processed by means of dynamic plastic deformation (DPD) at room temperature. Prior to the treatment, the initial material was annealed at 823 K for 40 min to obtain a relaxed coarse-grained state. Details of the DPD process can be found in previous works [3,13]. In this work, the sample was placed on a lower anvil and impacted by an upper anvil. Each single impact produced a height reduction of $\sim$2 mm and the final height of the sample reached $\sim$10 mm after multiple impacts. Therefore, the total plastic strain (ε) was $\sim$1 by defining $\varepsilon = \ln(H_0/H_f)$, where H_0 and H_f were the initial and the final sample heights, respectively. Disc samples of 10 mm in diameter and 1.8 mm in thickness were cut by electro-spark discharge from the longitudinal section containing the compression axis. After carefully cleaning, one surface of the specimen was polished to a mirror-like quality.

A commercial ^{63}Ni radioisotope available in HCl solution was deposited by drying 5 µl dilute solution ($\sim$4 kBq µl^{-1}) onto the polished surface. Each sample was sealed in a silica tube in purified Ar atmosphere and submitted to diffusion annealing (as given in Table 1). Temperatures were measured and controlled by a Ni–NiCr thermocouple with an accuracy of $\pm$1 K. After annealing treatments, samples were reduced in diameter by $\sim$1 mm in order to eliminate confounding effects from surface or lateral diffusion.

Table 1. Parameters of ^{63}Ni radiotracer diffusion in DPD Ni.

Sample no.	T (K)	t (s)	$\sqrt{D_V t}$ (nm)	D_{eff} (m^2 s^{-1})	D_{LGB} (m^2 s^{-1})
T385	385	3.42×10^5	8.5×10^{-10}	6.37×10^{-18}	2.52×10^{-19}
T428	428	3.40×10^5	6.6×10^{-8}	1.71×10^{-17}	3.47×10^{-19}
T458	458	3.06×10^5	8.1×10^{-7}	2.58×10^{-17}	5.14×10^{-19}
T489	489	2.61×10^5	7.5×10^{-6}	4.16×10^{-17}	1.68×10^{-18}
T513	513	6.26×10^4	1.8×10^{-5}	9.92×10^{-17}	2.34×10^{-18}

Note: D_V is the lattice diffusion coefficient in the coarse-grained sample extrapolated from the work by Maier et al. [14].

Diffusion penetration profiles were determined by the serial-sectioning technique using a precision parallel grinder. The section thickness (or penetration depth) was determined with an accuracy $<$0.1 µm from the density and the mass difference before and after each sectioning. The tracer concentration in a section is proportional to the relative specific radioactivity, that is, the counting rate after background subtraction divided by the section mass. The relative activity of ^{63}Ni radiotracer in each section was measured by a PerkinElmer TRI−CARB 2910 TR liquid-scintillation analyzer.

The microstructure of the DPD samples was characterized by scanning electron microscopy applying electron back-scattering diffraction (EBSD) analysis and by transmission electron microscopy (TEM). The EBSD was conducted on an FEI Nova NanoSEM 230 unit equipped with a field emission gun. A step size of 60 nm was used. For the statistics of misorientation angles across different grain/cell boundaries, any point pair with misorientation exceeding 2° was considered as a boundary. Detailed microstructures were examined by an FEI Tecnai F20 TEM operated at 200 kV. And the geometric phase analysis was applied to determine the atomic level strains in high-resolution TEM (HRTEM) images, following the experimental process in Ref. [15]. Foils were mechanically thinned and electropolished in an electrolyte of 10 vol.% perchloric acid and 90 vol.% ethanol at −20°C.

Results and discussion

A large amount of LAGBs (with misorientations within 2−15°) was noticed from the misorientation distribution measured by means of EBSD, as shown in Figure 1(a). This fact has been confirmed by convergent beam electron diffraction analyses in TEM, too [3]. By mapping a total area of $\sim$20,000 µm^2, the fraction of LAGBs was estimated to be $\sim$87%. From the TEM image in Figure 1(b), the lamellar grains formed by intersecting LAGBs are typically $\sim$200 and $\sim$500 nm along the short and long axes, respectively. Moreover, extremely high dislocation densities exist in the lamellar grains. Quantitative microstructural analyses in a previous work [3]

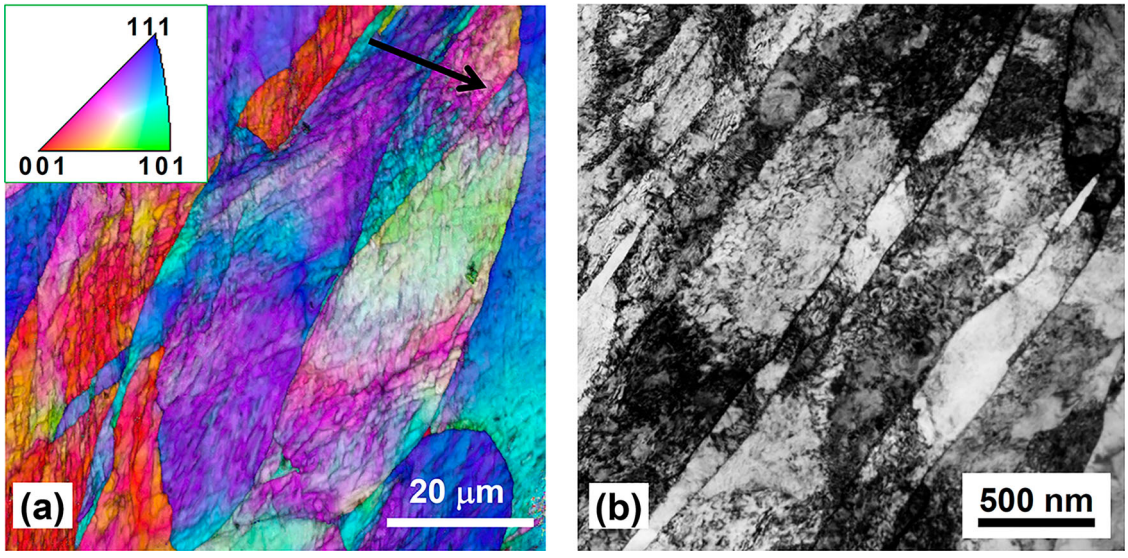


Figure 1. Representative (a) EBSD and (b) bright-field TEM images of the DPD Ni sample. The arrow in (a) shows the deformation direction.

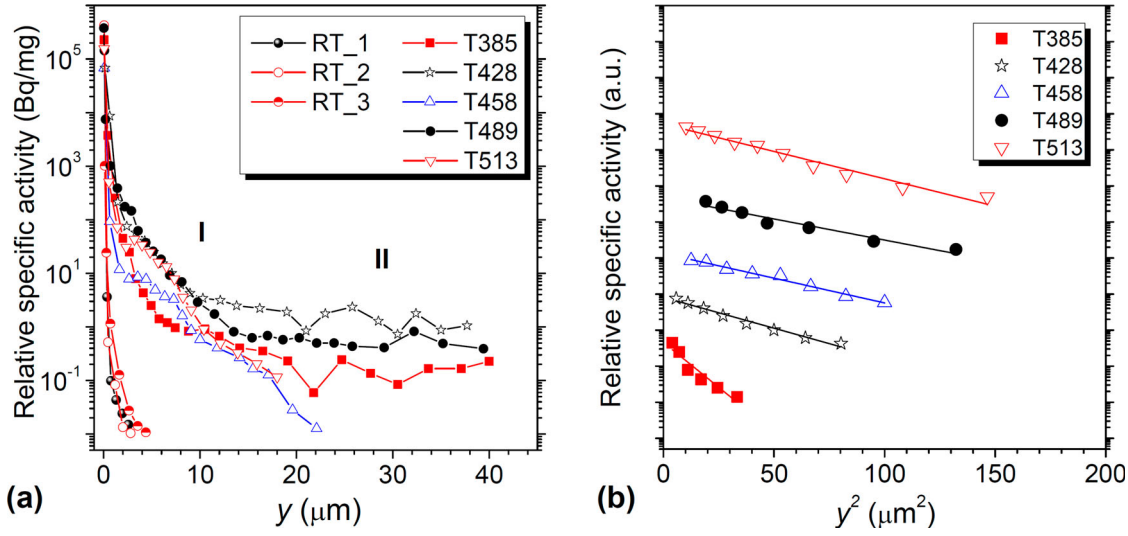


Figure 2. (a) Measured concentration profiles in DPD Ni samples subjected to different diffusion treatments (see Table 1), in comparison with 'zero' profiles (see text). (b) Diffusion profiles in Stage I in (a) are replotted in the log $\bar{C} - y^2$ coordinates according to Equation (1). The profiles in (b) are shifted along the ordinate axis (with $\bar{C}$ values rescaled) for a better clearness.

showed that the structural evolution during DPD follows a hierarchical pattern from the formation of cells and cell blocks to a lamellar structure, similar with that in metals deformed by conventional deformation processes. However, the dislocation density is significantly increased and the distance between boundaries is decreased due to the high strain rates (10^2–10^3 s^{-1}) during DPD.

While extra free volume and vacancy-like defects might form a more open structure of interfaces and even induce porosity in some metals processed by SPD [11,12], this possibility was carefully checked by measuring 'zero' profiles of ^{63}Ni (with β-quanta) and ^{110m}Ag (with γ-quanta) radiotracers in the DPD sample before and after diffusion annealing (i.e. the penetration profiles induced solely by tracer application without any diffusion annealing treatment were measured. In earlier works it was shown that this method reveals unambiguously the existence of interconnected porosity, e.g. in SPD Cu and Cu-based alloys [16,17]). As shown in Figure 2(a), the specific radioactivity values of ^{63}Ni decreases sharply to the background value ($< 3 \times 10^{-2}$ Bq mg^{-1}) at a depth of $\sim$3 μm in the as-DPD sample (RT_1) and the DPD

sample annealed at 385 K for 95 h (RT_2). By applying the more sensitive γ-quanta of ^{110m}Ag tracer, no radioactivity was detected in the section at a comparable depth (RT_3) either. Therefore, the existence of a percolating porosity can safely be excluded in the DPD Ni before and after diffusion annealing. The penetration of tracers definitely reflects diffusion along interfaces while probable lattice diffusion contribution is negligible ($\sqrt{D_v t} \ll 1$ nm, see Table 1).

The penetration profiles measured in DPD samples after different diffusion treatments are compared in Figure 2(a). Usually, the first several points close to the surface should be disregarded since they are associated with the remnant radioactivity of the deposited radioisotope layer and slight deviations from the parallel alignment of the sample surface on the abrasive foil. It is clear that the Ni tracer has remarkably penetrated into the DPD samples after the diffusion treatments. In addition, a two-stage penetration is observed on several profiles (marked as I and II on Figure 2(a)). The Stage II is possibly related to the ultrafast diffusion kinetics similar to that observed previously in SPD metals [18–20], that is, due to the diffusion-connection of 'open-channels' with segments of concentrated excess free volume [21] or interface migration [20,22,23] during annealing. The present work will focus on Stage I.

According to the classical solution of the diffusion equation for one-dimensional diffusion along the $y-$axis into a semi-infinite body, the effective interfacial diffusivity, D_{eff}, may be determined from the diffusion profiles as

$$D_{\text{eff}} = \frac{1}{4t}\left(-\frac{\partial \ln \bar{C}}{\partial y^2}\right)^{-1}, \qquad (1)$$

while the lattice diffusion is negligible. Here $\bar{C}$ is the nominal solute concentration (which is proportional to the measured relative specific radioactivity), and t is the diffusion time. The measured diffusion profiles are replotted in the $\log \bar{C} - y^2$ coordinates in Figure 2(b). It is clear that the concentration profiles can be well fitted by linear regression lines. Therefore, the effective interfacial diffusivities at different temperatures can be determined, as listed in Table 1 and shown in Figure 3. For comparison, the self-diffusivities along high-angle GBs (HAGBs) in the relaxed coarse-grained Ni [24] and the ultra-fine-grained Ni prepared by equal-channel angular pressing (ECAP) [11] are also included. It is noticeable that the effective interfacial diffusivity in DPD Ni is by more than 2 orders of magnitude higher than the GB self-diffusion rate in coarse-grained Ni.

Significantly enhanced interfacial diffusion kinetics have previously been observed in nanostructured materials produced by different SPD routes [5,10,11,18,25].

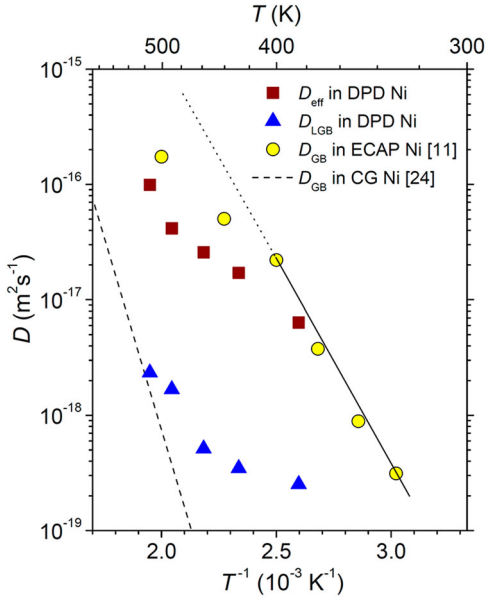


Figure 3. Comparison of the effective self-diffusion coefficients in DPD Ni with ECAP [11] and coarse-grained [24] Ni. The diffusion coefficients along LAGBs in DPD Ni are derived from Equation (3) according to an out-diffusion model from HAGBs to LAGBs.

This was attributed to a deformation-modified state of GBs, which accumulate a large number of extrinsic dislocations and possess higher free energy in comparison with conventional GBs in coarse-grained samples. For example, the excess free energy of HAGBs in ECAP Ni was estimated to be 30% higher than that in annealed coarse-grained Ni [11], and the excess free energies of GBs and TBs in Cu samples processed by DPD and surface mechanical attrition treatment were also significantly enhanced [5,10].

In comparison with the diffusivity along deformation-modified GBs in ECAP Ni, the effective interfacial diffusivity in DPD Ni appears to be remarkably lower. The possibilities related to this difference will be considered in the following.

Accelerated relaxation of the deformation-modified state of HAGBs

The deviation from a linear Arrhenius dependence for GB diffusion in ECAP Ni at temperatures higher than 400 K (see Figure 3) was related to the relaxation of the deformation-modified state [11]. The relaxation time (τ) of an array of extrinsic GB dislocations, which contribute to the deformation-modified state, can be estimated as [21,26]:

$$\tau = \frac{kTd^3}{A\delta D_{\text{GB}}^{Rel} G\Omega}, \qquad (2)$$

where d is the average grain size, k is Boltzmann's constant, A is a geometrical factor, δ is the diffusional GB width, G is the shear modulus, Ω is the atomic volume, and D_{GB}^{Rel} is the self-diffusivity along relaxed GBs. While the spacing between HAGBs in the DPD sample is much larger than that in the ECAP sample, and other parameters are similar in both samples, the relaxation time of deformation-modified HAGBs in DPD Ni is expected to be slower, and the measured effective diffusion coefficients should be higher. Therefore, this possibility is not applicable to the present case.

Effect of dislocation rearrangement or recrystallization

Microstructure recovery or recrystallization is expected to occur during diffusion annealing thereby decreasing the mean diffusivity, especially at higher temperatures. However, the microstructure stability in nano-laminated or UFL samples with mostly LAGBs is much higher than that of conventional nanograined or ultra-fine-grained samples. For example, the onset temperature for lamellae thickening is ~779 K (for 1 h) in nano-laminated Ni. In comparison, the onset temperature for significant grain coarsening in nanograined Ni with mostly HAGBs is ~716 K [4]. In addition, the influence of dislocation rearrangements and/or GB migration on diffusion kinetics has been investigated in previous works. The results suggested a linear dependence of $\log \bar{C}$ on y in both cases [19,21], while $\log \bar{C}$ seems to depend linearly on y^2 instead of required y^1-dependence for the considered scenario in the present work (see Figure 2(b)).

Out-diffusion from HAGBs to LAGBs

As shown in Figure 1, the DPD Ni is typically characterized by a hierarchic microstructure, that is, the cells enclosed by HAGBs are separated by grains formed from intersecting LAGBs. The leakage of the Ni tracer from HAGBs into LAGBs is expected to decrease the apparent diffusivity, and the diffusion problem corresponds to the so-called C-B kinetic regime after Divinski's classification [5,6]. In this case, the diffusion rate along HAGBs is characterized by the value $P_{HGB} = \delta_{HGB} D_{HGB}/\chi$,

$$P_{HGB} = 1.322\sqrt{\frac{D_{LGB}}{t}}\left(-\frac{\partial \ln \overline{C}}{\partial y^{6/5}}\right)^{-5/3}, \qquad (3)$$

where δ_{HGB} is the width of HAGBs (measured to be ~0.5 nm [24,27]), D_{HGB} and D_{LGB} are the diffusion coefficients along HAGBs and LAGBs, respectively. χ denotes the volume fraction of the sites where LAGBs cross HAGBs, that is,

$$\chi = \frac{\delta_{LGB}}{2d_s} + \frac{\delta_{LGB}}{2d_l}, \qquad (4)$$

where δ_{LGB} is the width of LAGBs (taken as 0.5 nm), d_s and d_l are the sizes of grains separated by LAGBs along the short and long axes, respectively. Considering

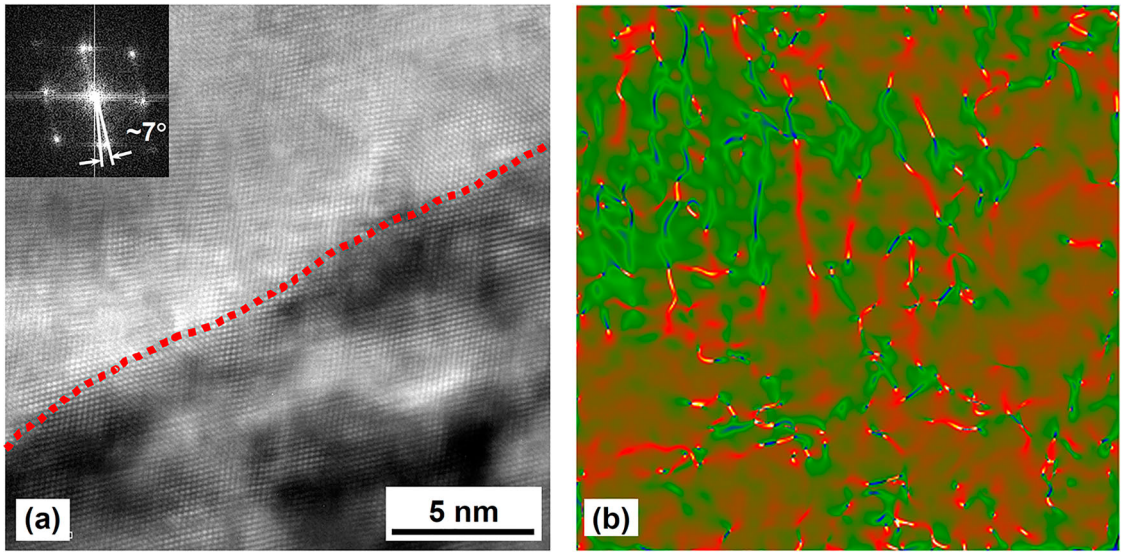


Figure 4. (a) An HRTEM image showing an LAGB separating two grains both oriented along the ⟨110⟩ direction. The inset indicates the corresponding Fourier transformation, by which the misorientation across the boundary is derived (~7°). (b) Strain mapping showing the shear strain component ε_{xy} in (a). 'Hot spots' correspond to dislocation cores. Details of the strain mapping method can be found in Ref. [15].

that the interfacial diffusivity in DPD Ni is very close to the previously measured self-diffusion coefficients along HAGBs in ECAP Ni [11] at lower homologous temperatures ($\sim$385 K), when the leakage of tracer from HAGBs to LAGBs in both samples is rather limited, one may assume HAGBs in DPD Ni and ECAP Ni have similar diffusion rates at the same temperature. However, it is crucial that the density of LAGBs is significantly lower and the corresponding cell size is larger in ECAP Ni than those in DPD Ni, so that the so-called C–C kinetic regime is promoted in the hierarchical microstructure of ECAP Ni [11]. Therefore, the self-diffusion coefficients along LAGBs in DPD Ni are determined following Equation (3), as presented in Table 1 and Figure 3.

It is noticed that the determined diffusivity along LAGBs in DPD Ni is even higher than the Ni self-diffusion coefficient corresponding to HAGBs in coarse-grained Ni, and therefore even slower diffusion values are expected for relaxed LAGBs in well-annealed coarse-grained Ni [28]. Correspondingly, an opposite trend would be expected due to a low excess free energy and the sessile intrinsic dislocations of LAGBs. However, LAGBs in DPD Ni might accumulate a large number of extrinsic GB dislocations and be associated with an extra free energy. As revealed in Figure 4, a high density of extrinsic GB dislocations co-exists with a boundary of $\sim$7°. While an increased density of edge dislocations can be identified in the vicinity of the boundary on the HRTEM image, their contribution to the misorientation is significantly smaller than the indicated value. Therefore, the LAGB should not be a pure tilt GB only composed of edge dislocations, and screw- and mixed-character dislocations have to exist, too, and contribute to the misorientation. According to the strain mapping results, the dislocation density in the LAGB vicinity is very roughly estimated to be $\sim 3 \times 10^{17}\,\mathrm{m}^{-2}$ (This value is most likely overestimated due to a lower quality of the HRTEM image owing significant residual strains induced by DPD). Further observations indicated that such dislocations are glissile and prone to rearrange and/or annihilate during annealing. Nevertheless, they will contribute to the significantly enhanced diffusion kinetics along LAGBs. For example, it was demonstrated that the pipe diffusion of impurity atoms along dislocations in Al needs a smaller activation energy and the diffusion rate is about three orders of magnitude higher than those of bulk diffusion [29]. And an enhancement of self-diffusion via pipe diffusion mechanism was documented for polycrystalline Ag [30]. In addition, the intensive interaction with dislocations can strongly modify the LAGB structure [31], induce even hexagonal dislocation networks. These features are known to strongly affect the GB diffusion rates even in annealed bicrystals [32].

In summary, UFL Ni with a large fraction ($\sim$87%) of LAGBs has been produced by means of DPD. The effective interfacial diffusivity in DPD Ni is more than 2 orders of magnitude higher than the GB diffusivity in coarse-grained Ni, but lower than the GB diffusivity in ECAP Ni. The out-diffusion from HAGBs to a LAGB network is discussed to slow down the effective diffusivity in DPD Ni. Such out-diffusion is suggested be significantly enhanced by a high density of deformation-induced extrinsic GB dislocations.

Acknowledgements

Authors are grateful to Dr M. Wegner for EBSD measurements and to Prof. H.W. Zhang for valuable discussion.

Disclosure statement

No potential conflict of interest was reported by the authors.

Funding

Z.B.W., Z.P.L., and K.L. acknowledge financial supports by the National Natural Science Foundation of China (grant number 51231006) and the National Key Research and Development Program of China (grant number 2017YFA0204400). Z.B.W. also acknowledges support by the Alexander von Humboldt Foundation. S.V.D. and G.W. gratefully acknowledge partial support by the Deutsche Forschungsgemeinschaft.

References

[1] Lu K. Stabilizing nanostructures in metals using grain and twin boundary architectures. Nature Rev Mater. 2016;1:16019.
[2] Lu K, Lu L, Suresh S. Strengthening materials by engineering coherent internal boundaries at the nanoscale. Science. 2009;324(5925):349–352.
[3] Luo ZP, Zhang HW, Hansen N, et al. Quantification of the microstructures of high purity nickel subjected to dynamic plastic deformation. Acta Mater. 2012;60(3):1322–1333.
[4] Liu XC, Zhang HW, Lu K. Strain-induced ultrahard and ultrastable nanolaminated structure in nickel. Science. 2013;342(6156):337–340.
[5] Wang ZB, Lu K, Wilde G, et al. Interfacial diffusion in Cu with a gradient nanostructured surface layer. Acta Mater. 2010;58(7):2376–2386.
[6] Divinski SV, Hisker F, Kang YS, et al. Ag diffusion and interface segregation in nanocrystalline gamma-FeNi alloy with a two-scale microstructure. Acta Mater. 2004;52(3):631–645.
[7] Würschum R, Farber P, Dittmar R, et al. Thermal vacancy formation and self-diffusion in intermetallic Fe3Si nanocrystallites of nanocomposite alloys. Phys Rev Lett. 1997;79(24):4918–4921.
[8] Harrison LG. Influence of dislocations on diffusion kinetics in solids with particular reference to alkali halides. Trans Faraday Soc. 1961;57(8):1191–2001.
[9] Divinski SV. Grain boundary diffusion in severe plastically deformed metals: state of the art and unresolved issues. Diffus Found. 2015;5:57–73.
[10] Wang HL, Wang ZB, Lu K. Interfacial diffusion in a nanostructured Cu produced by means of dynamic plastic deformation. Acta Mater. 2011;59(4):1818–1828.

[11] Divinski SV, Reglitz G, Rosner H, et al. Ultra-fast diffusion channels in pure Ni severely deformed by equal-channel angular pressing. Acta Mater. 2011;59(5):1974–1985.
[12] Sauvage X, Wilde G, Divinski SV, et al. Grain boundaries in ultrafine grained materials processed by severe plastic deformation and related phenomena. Mater Sci Eng A. 2012;540:1–12.
[13] Li YS, Tao NR, Lu K. Microstructural evolution and nanostructure formation in copper during dynamic plastic deformation at cryogenic temperatures. Acta Mater. 2008;56(2):230–241.
[14] Maier K, Mehrer H, Lessmann E, et al. Self-diffusion in nickel at low-temperatures. Phys Status Solidi B. 1976;78(2):689–698.
[15] Wilde G, Ribbe J, Reglitz G, et al. Plasticity and grain boundary diffusion at small grain sizes. Adv. Eng. Mater. 2010;12(8):758–764.
[16] Ribbe J, Baither D, Schmitz G, et al. Network of porosity formed in ultrafine-grained copper produced by equal channel angular pressing. Phys Rev Lett. 2009;102(16):165501.
[17] Ribbe J, Baither D, Schmitz G, et al. Ultrafast diffusion and internal porosity in ultrafine-grained copper-lead alloy prepared by equal channel angular pressing. Scripta Mater. 2009;61(2):129–132.
[18] Amouyal Y, Divinski SV, Estrin Y, et al. Short-circuit diffusion in an ultrafine-grained copper-zirconium alloy produced by equal channel angular pressing. Acta Mater. 2007;55(17):5968–5979.
[19] Ribbe J, Schmitz G, Rosner H, et al. Effect of back pressure during equal-channel angular pressing on deformation-induced porosity in copper. Scripta Mater. 2013;68(12):925–928.
[20] Prokoshkina D, Klinger L, Moros A, et al. Effect of recrystallization on diffusion in ultrafine-grained Ni. Acta Mater. 2014;69:314–325.
[21] Divinski SV, Reglitz G, Golovin IS, et al. Effect of heat treatment on diffusion, internal friction, microstructure and mechanical properties of ultra-fine-grained nickel severely deformed by equal channel angular pressing. Acta Mater. 2015;82:11–21.
[22] Wang ZB, Lu K, Wilde G, et al. Effects of grain growth on interface diffusion in nanostructured Cu. Scripta Mater. 2011;64(11):1055–1058.
[23] Klinger L, Rabkin E. A model of grain boundary diffusion in polycrystals with evolving microstructure. Int J Mater Res. 2009;100(4):530–535.
[24] Divinski SV, Reglitz G, Wilde G. Grain boundary self-diffusion in polycrystalline nickel of different purity levels. Acta Mater. 2010;58(2):386–395.
[25] Wang ZB, Lu K. Diffusion and surface alloying of gradient nanostructured metals. Beilstein J Nanotechnol. 2017;8:547–560.
[26] Nazarov AA, Romanov AE, Valiev RZ. On the structure, stress-fields and energy of nonequilibrium grain-boundaries. Acta Metall Mater. 1993;41(4):1033–1040.
[27] Prokoshkina D, Esin VA, Wilde G, et al. Grain boundary width, energy and self-diffusion in nickel: effect of material purity. Acta Mater. 2013;61(14):5188–5197.
[28] Paul A, Laurila T, Vuorinen V, et al. Thermodynamics, diffusion and the Kirkendall effect in solids. Heidelberg: Springer; 2014. p. 522.
[29] Legros M, Dehm G, Arzt E, et al. Observation of giant diffusivity along dislocation cores. Science. 2008;319:1646–1649.
[30] Sommer J, Herzig C. Direct determination of grain-boundary and dislocation self-diffusion coefficients in silver from experiments in type-C kinetics. J Appl Phys. 1992;72:2758–2766.
[31] Liu B, Raabe D, Eisenlohr P, et al. Dislocation interactions and low-angle grain boundary strengthening. Acta Mater. 2011;59:7125–7134.
[32] Budke E, Surholt T, Prokofjev SI, et al. Tracer diffusion of Au and Cu in a series of near Sigma = 5 (310)[001] symmetrical Cu tilt grain boundaries. Acta Mater. 1999;47:385–395.